Modeling the Thermal Fields of Deposited Materials During the Spray Rolling Process

FENGXIAN LI, YUNZHONG LIU, and JIANHONG YI

The technology of spray rolling can be applied to manufacture strips with a uniform cooling rate and a high production rate. The cooling behavior of the spray-rolled material prior to rolling contact was studied using mathematical models, tracing the accumulation of multi-layers with respect to time. Thermal history, elastic–plastic, and friction behavior of the material were considered in the complicated rolling process. The developed model had a good agreement with experimental results with potential to be utilized for prediction of the spray-rolled material thermal profile. Results show that the temperature of deposited materials prior to/or during rolling and the total equivalent plastic strain distribution in the deformation zone of deposited materials during rolling increase with increasing roller preheating temperature, the initial droplet temperature, and the mass flux distribution of the spray cone. Moreover, the deposit thickness and enthalpy remaining in the deposit are found to be the dominant influencing factors on the thermal field of deposited materials during the spray rolling process.

I. INTRODUCTION

SPRAY rolling is a novel metallic semi-solid near-net-shape forming technique. It was proposed and invented by McHugh et al.[1] He later established cooperation with Lavernia and coworkers[1,2] on the development of spray rolling process and material investigation. Spray rolling combines the advantages of twin-roll casing and spray forming in a single operation, benefiting industry through less energy consumption and reduced scrap formation making strip production cost effective.

In spray rolling (Figure 1), the molten metal stream is atomized into disintegrated micro-sized droplets by an inert gas and deposited on the roller surface. Then the deposited material is dragged into the roll gap and consolidated to a full dense strip. Obviously, cooling and solidification of the molten metal occur in three successive stages: during the flight, prior to rolling contact and during rolling. The metallurgical quality of the spray-rolled strip, e.g., porosity and segregation, microstructure, is always determined by the cooling and solidification behavior of the spray-rolled material. Therefore, modeling of the thermal history of the preform during spray rolling is an important topic for better understanding of the process, and it also helps the finding of optimal processing conditions for high quality strip products.

The heat flow and solidification of various spray formed preforms have been investigated extensively.[3–10]

In the thermal dynamic models, the physical processes were often modeled using simplified assumptions, i.e., assuming a constant convective heat transfer coefficient at the preform surface and substrate surface, no droplet redeposition. These assumptions may render a limited accuracy when calculating the heat flow and solidification of the spray-rolled materials. Moreover, it should be noted that the previous work on spray forming focused on deposits only in the shape of a billet, tube, or ring.[6–8] In spray rolling, the changes of thickness, temperature, and microstructure of deposited materials at different positions are noticeable, and the thermal condition is much affected. For example, rollers collect spray, extract remaining latent heat, and consolidate semi-solid material to form a fully-dense strip that makes material behavior in the rolling process complicated. These make simulation study of the thermal dynamics during the spray rolling process a challenging task. Lin et al.[11,12] studied the mechanism that controls the maximum and minimum deposition rate during the spray rolling process. However, limited studies have been carried out to reveal the cooling and solidification behavior of the deposited material prior to and during rolling process. In our previous work, the deposit shape during the spray rolling process was modeled.[13]

Based on our previous work,[13] the solidification behavior of the deposited material prior to rolling and during rolling are investigated in this study. The heat-transfer models of the deposited material have been established to represent the complex thermal field during the spray rolling process. In comparison with previous work on the simulation of spray forming process,[6–8] (1) the process of deposition was treated as accumulation of multi-layers with respect to time; (2) this model considers the effect of thermophysical properties of the material on solidification behavior, and physics such

FENGXIAN LI, Ph.D. Researcher, and JIANHONG YI, Professor, are with the Kunming University of Science and Technology, Kunming 650093, P.R. China. Contact e-mail: 175182344@qq.com YUNZHONG LIU, Professor, is with the South China University of Technology, Guangzhou 510640, P.R. China.
Manuscript submitted June 12, 2013.
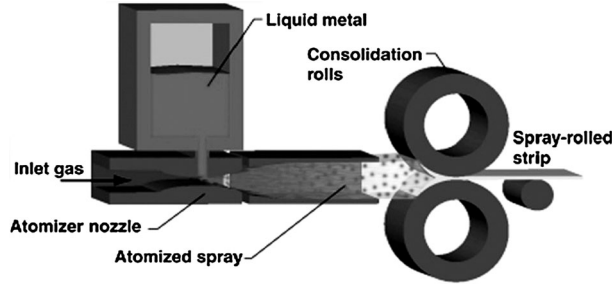Article published online May 21, 2014.

Fig. 1—Schematic of spray rolling.[1]

as elastic–plastic dynamics and friction; (3) generic algorithms of coupling of temperature field and strain field were developed for the rolling stage.

II. MODELING

A. Cooling Behavior of the Deposited Material Prior to Rolling Contact

The heat flow inside the deposit prior to rolling is generally a transient, non-liner heat conduction event that includes release of latent heat during solidification. The governing heat equation is:[14]

$$\rho\left(C_d \frac{dT}{dt} - \Delta H_d \frac{df_s}{dt}\right) = \frac{1}{r}\left(\frac{\partial}{\partial x}\left(Kr\frac{\partial T}{\partial x}\right) + \frac{\partial}{\partial r}\left(Kr\frac{\partial T}{\partial r}\right)\right),$$
[1]

where T is the temperature of the deposit, t is time, x and r are the axial distance and the radius, respectively, $C_d = C_l \times f_l + C_s \times f_s$, $\Delta H_d = \Delta H_f - (C_l - C_s)(T_l - T)$, here, C_d, C_l, C_s are the heat capacities per unit mass of liquid–solid mixture, liquid and solid, respectively, f_l and f_s are the liquid and solid fraction, T_l is the liquidus temperature of the alloy, ΔH_f is the latent heat per unit mass, ρ is the density, K is the heat conductivity.

For the 7050 aluminum alloy, the Scheil function is often adopted to relate the alloy liquid fraction to temperature during solidification:[15]

$$f_l = \left(\frac{T - T_s}{T_l - T_s}\right)^{\left(\frac{1}{1-ke}\right)},$$
[2]

where T_s is the solidus temperature of the alloy, and ke is a partition coefficient.

$$\frac{df_l}{dT} = \frac{1}{(1 - ke)(T_l - T_s)}\left(\frac{T - T_s}{T_l - T_s}\right)^{\frac{ke}{1-ke}}.$$
[3]

By defining a term "equivalent specific heat" C_{zong} as:

$$C_{zong} = C_d + \Delta H_d \frac{df_l}{dT} = [C_s - (C_s - C_l)f_l]$$
$$+ [\Delta H_f - (C_l - C_s)(T_l - T_d)]\frac{df_l}{dT}.$$
[4]

Figure 2 shows the calculated fraction of solid and the heat capacity over the temperature range of 780 K to
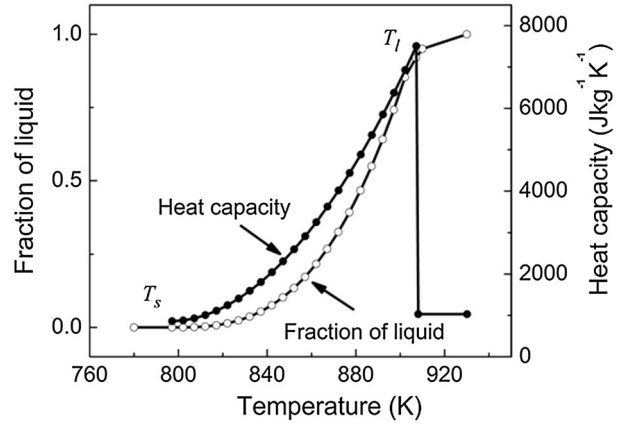

Fig. 2—The fraction of liquid and heat capacity of 7050 aluminum alloy as a function of temperature.

Table I. Thermophysical Properties of 7050 and Rollers[16]

7050 Aluminum alloy		
Heat capacities per unit mass (solid)	C_s	860 J kg^{-1} K^{-1}
Heat capacities per unit mass (liquid)	C_l	1029 J kg^{-1} K^{-1}
Thermal conductivity	K	154 W m^{-1} K^{-1}
Liquid temperature	T_l	908 K (635 °C)
Solid temperature	T_s	797 K (524 °C)
Latent heat of fusion	ΔH_f	257,500 J kg^{-1}
Low carbon steel		
Heat capacities per unit mass	C_{roll}	635 J kg^{-1} K^{-1}
Density	ρ_{roll}	7874 kg m^{-3}
Thermal conductivity	K_{roll}	46 W m^{-1} K^{-1}

920 K (507 °C to 647 °C) using Eqs. [2] through [4] with further details given in Table I.

The heat flow insider the roller involves transient heat conduction without solidification, and is governed by:

$$\rho_{roll}C_{roll}\frac{dT}{dt} = \frac{1}{r}\left(\frac{\partial}{\partial x}\left(K_{roll}x\frac{\partial T}{\partial x}\right) + \frac{\partial}{\partial r}\left(K_{roll}r\frac{\partial T}{\partial r}\right)\right),$$
[5]

where ρ_{roll} is the density of roller, C_{roll} is the specific heat of roller, K_{roll} is the heat conductivity of roller. All the coefficient bear the same meaning as those in Eq. [1] but refer to the roller using the subscript "roll". The thermal properties of the low carbon steel roller used in the simulation are also listed in Table I.[16]

At the deposit surface, the heat flux q_{con} due to gas convective can be expressed as:

$$q_{com} = h_g(T - T_g),$$
[6]

where T_g is the gas temperature, h_g is the convective heat transfer coefficient at the deposit/gas interface in spray rolling.

The heat flux q_{em} from the preform surface to the environment by radiation can be written as:

$$q_{em} = \sigma\varepsilon(T^4 - T_\infty^4),$$
[7]

where ε is the constant emissivity of the preform surface, σ is the Stefan–Boltzmann constant (5.6697×10^{-8} W m^{-2} K^{-4}), T_∞ is the temperature of the wall of the spraying chamber.

At the deposit-roller interface, the heat flux q_{int} between the preform and roller can be expressed as follows:

$$q_{int} = h_{int}(T - T_{roll}), \qquad [8]$$

where T and T_{roll} are the temperatures of the interface at the preform side and at the roller side, respectively, h_{int} is interfacial heat transfer coefficient, accounting for the conductive, convective, and radiation heat transfer across the interface.

If a part of the roller surface was exposed to an external heat source, the heat flux from the substrate to the environment by convection and radiation is determined by:

$$q_{roll} = h_g(T - T_g) + \sigma\varepsilon(T^4 - T_\infty^4). \qquad [9]$$

Because spray processing parameters in spray rolling are in a range similar to those in spray forming, thus the heat transfer coefficient at the deposit/gas interface, roller, and/or deposit surface during spray rolling is comparable with that at the deposit/gas interface, substrate, and/or deposit surface during spray forming. Consequently, the convective heat transfer coefficient h_g at the deposit/gas interface in spray rolling could be considered 100 W m^{-2} K^{-1}, and similar to heat transfer coefficient h_{roll} at the roller surface. Moreover, the heat transfer coefficient h_{int} (W m^{-2} K^{-1}) at the deposit/substrate interface during spray rolling can be expressed using the following exponential function: $h_{int} = 45 \times 10^3 \exp(-10t) + 5 \times 10^3$.[17]

B. Cooling Behavior of the Deposited Material During Rolling

The solidification behavior of the deposited material during rolling is a thermo-mechanical process, which requires the heat conduction equation and deformation for analysis. The equations governing thermo-mechanical deformation are summarized as: Reference for this equation is required.[18]

$$Q + K_c\left(\frac{\partial^2 T}{\partial x^2} + \frac{\partial^2 T}{\partial r^2}\right) - \rho C\frac{\partial T}{\partial t} = 0, \qquad [10]$$

where K_c the thermal conductivity and Q is the heat generation term representing the heat released due to plastic work. The heat generation is calculated using Eq. [11]:

$$Q = K_p \cdot \bar{\sigma} \cdot \bar{\varepsilon}, \qquad [11]$$

where K_p is the efficiency of conversion of plastic work into heat, which is assumed to be about 0.9 for 7050 aluminum alloy, $\bar{\sigma}$ is the equivalent stress, and $\bar{\varepsilon}$ is the equivalent strain rate.

During the rolling stage, the deposited material under an external rolling pressure condition is more compact

than that in the initial instant of the droplet deposition. Due to the plastic deformation and friction at the contact surface, the heat will be generated when the rolled strip enters into the deformation region.

For the interstand cooling, heat loss is calculated in a standard manner:

$$q_1 = h_r(T - T_a) + \sigma\varepsilon(T^4 - T_a^4), \qquad [12]$$

where T_a is the ambient temperature, the value of convection coefficient h_r 25 W m^{-2} K^{-1} has been determined by experience.

Contact heat loss model used is expressed as:

$$q_2 = h_c(T - T_a), \qquad [13]$$

where h_c is the convection coefficient. Interfacial contact during rolling in spray rolling is similar to that during twin-rolling casting. Thus, the interfacial heat transfer coefficient during rolling in spray rolling is comparable with that during twin-roll casting. Consequently, the interfacial heat transfer coefficient at the deposit/roller interface was determined as 5×10^4 W m^{-2} K^{-1} according to that during twin-roll casting.[19,20]

The friction heat q_3 between strip and roll is written as:

$$q_3 = K_f \cdot |\tau \cdot \Delta v|, \qquad [14]$$

where τ is the friction force, Δv is the roller-plate relative velocity, and K_f is the distribution coefficient of heat. In this case, K_f is equal to 0.5.

C. Numerical Implementation

For deposition of 7050 aluminum alloy on two tool steel mandrels with a diameter of 0.2 m, a fixed roll gap of 0.004 m, rolling at 3.14 rps, and a spray distance of 0.4 m, a maximum mass flux (m) of 30 and 50 kg m^{-2} s^{-1}, as a baseline case, the cross-sectional final shapes of a deposit under a steady state obtained by simulation are shown in Figure 3, which has been verified by the experimental results and strip production rate in Reference 13. The performance of the deposited material on the surface of the rollers maintains its top surface profile, *i.e.*, it has settled to a steady-state condition. Obviously, the deposit thickness and size increase gradually with increasing rotational angle. This is expected, due to the position closer to the spray axis gaining more material per unit time and therefore, the trajectories are increasing more quickly toward the spray axis.

We can calculate the cooling and solidification behavior of the deposited material prior to rolling through "layered method" with respect to time. Figure 4(a) (left) highlights three mesh layers, the roller surface, the first and second layers of deposited material in a time interval. First, a layer of material is deposited on the roller surface. The temperatures of the first deposited layer and roller surface changed. When the second layer of deposited material was added on the first one, part of the second layer was deposited directly on roller surface due to rotation of the first layer. This is similar to that of the first layer at this position, thus it is reasonable to
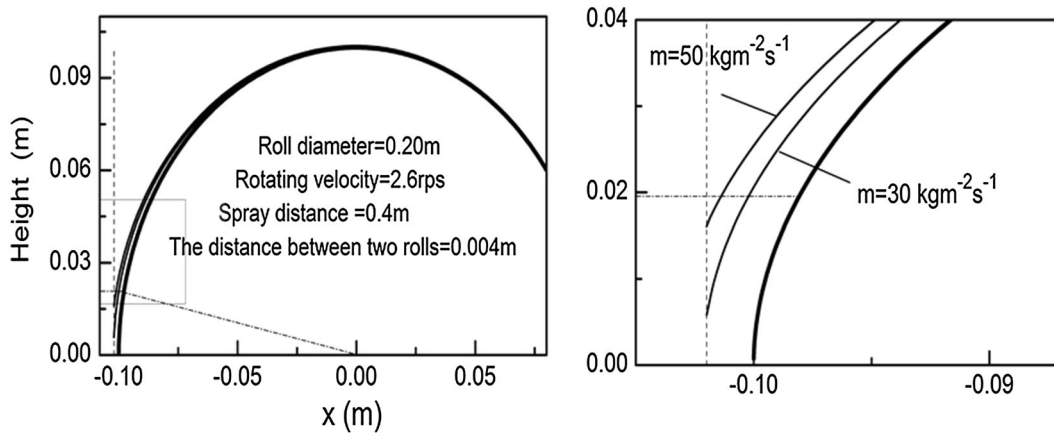
Fig. 3—Shape evolution through the longitudinal section of a deposit at maximum mass flux of 30 and 50 kg m^{-2} s^{-1}.[13]

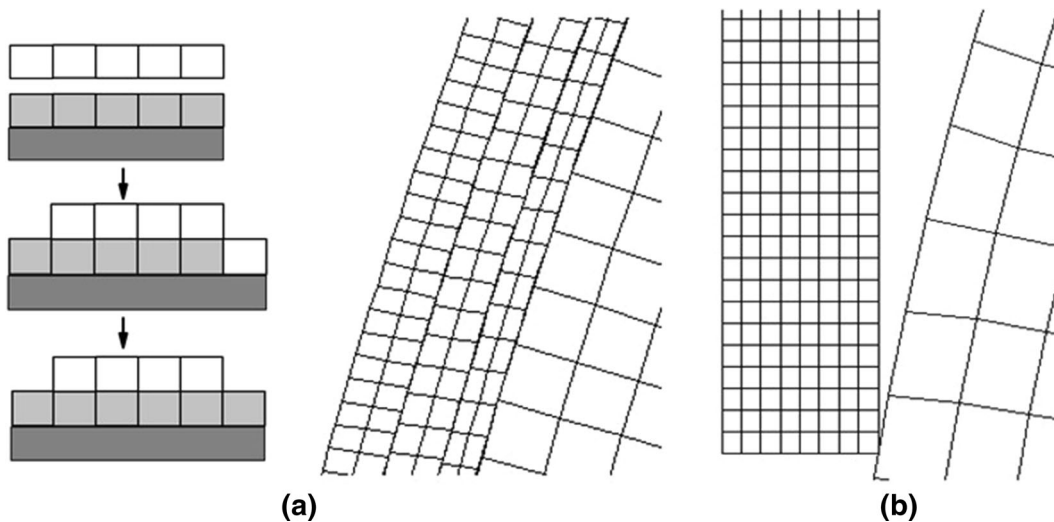**(a)**   **(b)**

Fig. 4—Schematic of the convective heat transfer profile at the deposit preform and roller surface, and meshes adopted for the deposit, the roll and the plate: [$m = 50$ kg m^{-2} s^{-1}, $T_{roll} = 320$ K (47 °C), and T_d 828 K (555 °C)]: (a) deposition stage; (b) rolling stage.

merge this part of the second layer into the first layer. Finally, the whole process of deposition during spray rolling can be treated as accumulation of multi-layers with respect to time. The two-dimensional mesh used in the analysis (Figure 4), was established using a commercial code Marc/Mentat. The definition of the element mesh foresees the discretization of the deposited materials and the roller (Figure 4(a) right), the plate and the roller (Figure 4(b)), and the schematization of the contact between the bodies.

For a control area (i, j) of size Δr by $\Delta \theta$ located in the computational domain, the energy conservation principle applied to the control area as a closed system gives:

$$\rho \left(C_d + \Delta H_d \frac{\partial f_1}{\partial t} \right) \frac{\partial T}{\partial t} = Q_1 + Q_2 + Q_3 + Q_4, \quad [15]$$

where $Q_1 = h_1 \times (T_{i,j+1} - T_{i,j})/\Delta r$, $Q_2 = h_2 \times (T_{i,j-1} - T_{i,j})/\Delta r$, $Q_3 = h_3 \times (T_{i+1,j} - T_{i,j})/\Delta r$, $Q_4 = h_4 \times (T_{i-1,j} - T_{i,j})/\Delta r$, represent the heat fluxes across the shared

interfaces between the control area and four neighboring control area.

A general purpose, proprietary finite-element software program, Marc/Mentat, has been used to develop a coupled thermo-mechanical model of the deformation processes occurring during the spray rolling of 7050 aluminum alloy. For the convenience of model establishment, some assumptions are made in the model as follows: the roll is considered as rigid material with the elastic deformation ignored. Two-dimensional FEM is used to build the analysis model. Therefore, the gradients of strain and temperature in the transverse direction are ignored. Considering the rolling symmetry in the thickness direction, only one work roll and one-half of the strips were modeled. Then generic algorithms of coupling of temperature field and strain field were developed according to these assumptions. An updated Lagrange procedure was used to account for large strain plasticity. An adaptive mesh was used due to the high deformation rate (Figure 5), with enthalpy and
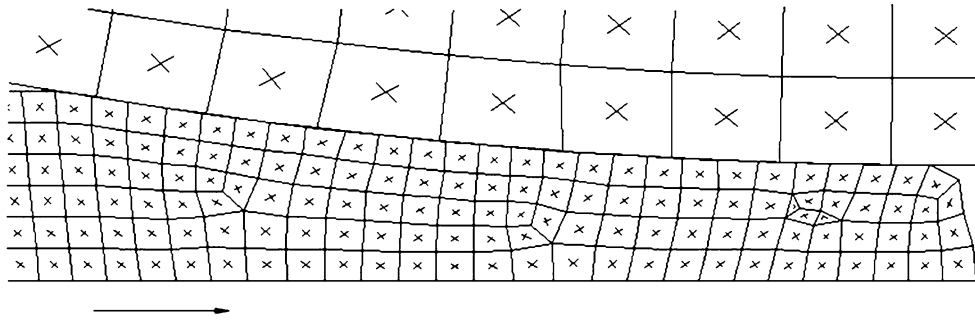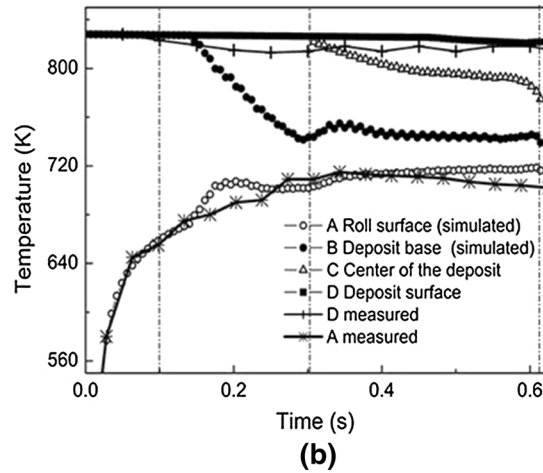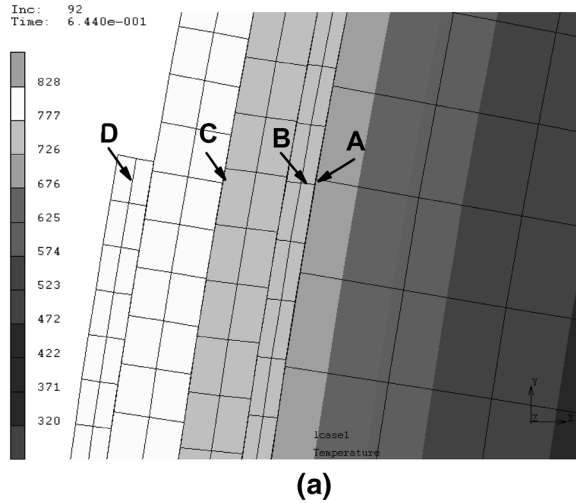
Fig. 5—Schematic of adaptive meshing methods.

(a)

(b)

Fig. 6—(*a*) Temperature distribution through the longitudinal section of a deposit at $m = 50$ kg m^{-2} s^{-1}, $T_{\text{roll}} = 320$ K (47 °C), and $T_{\text{d}} = 828$ K (555 °C), and (*b*) thermal histories at different locations including experimental results.

temperature at each mesh node conservatively transferred onto the new mesh in the next time step.

During the spray rolling process, physical property data (specific heat, thermal conductivity, thermal expansion coefficient, and Young's modulus) and their variation with temperatures were obtained from publications provided by Battle.[16] Under the standard spray rolling condition, the preheating temperature of the roller T_{roll}, the atomizing gas temperature T_{g}, the temperature of the spray chamber wall T_{w} are 320 K, 500 K, and 550 K (47 °C, 227 °C, and 277 °C), respectively. Since the temperature of impinging droplets T_{d} is affected by the cooling process during flying and droplets of different sizes, for simplicity, the average temperature of droplets with a mass median diameter arrived at the substrate is selected as an initial droplet temperature in present simulation, which can be determined based on our previous work.[21] For deposition of 7050 aluminum alloy on two tool steel mandrels with a maximum mass flux (m) of 50 kg m^{-2} s^{-1}, the initial droplet temperature is determined as 828 K (555 °C) at a spray distance of 0.4 m.[21]

Then, the corresponding entry angle and the temperature profile of the deposited material prior to rolling were utilized to be the initial conditions of rolling. To verify the

temperature evolution, the temperatures of the deposit at various locations on the preform surface were measured using an infrared radiation thermometer and /or a contact pyrometer. In order to reveal the effect of processing parameters on the thermal profiles of a spray-rolled material, variations of process parameters have also been made with respect to different thermal states. These variations will be discussed in the following section.

III. RESULTS

A. *Cooling Behavior of the Deposited Material Prior to Rolling Contact*

For deposition of 7050 aluminum alloy on two tool steel mandrels with a maximum mass flux of 50 kg m^{-2} s^{-1}, a substrate temperature of 320 K (47 °C) and an initial droplet temperature of 828 K (555 °C),[21] the temperature profiles of the deposit and the roller were estimated by simulation, and revealed by the color map (Figure 6(a)). Since the atomizing gas is spraying toward the preform, the highest temperature is found to be in the middle of the left slop of the deposit. Since the deposited layer will cool down by heat transfer to the

environment and the roller, the surface temperature of the deposit decreases faster from the centerline of the spray cone to the edge.

Thermal histories at four representative positions, *i.e.*, roller surface, deposit base, center of the deposit, and deposit surface are shown in Figure 6(b), respectively. For measurement positions B and C, the temperature data are plotted after 0.15 and 0.31 seconds, respectively. This considers that it takes some time till a layer of deposited material is added. The surface temperature of the roller (point A) increases gradually from 320 K to 701 K (47 °C to 428 °C) in 0.31 seconds because deposition of high temperature particles. Conversely, the cooling curve of deposited material at the interface (point B) decreases firstly owing to the cooling of atomizing gas and heat loss from the roller. Subsequent deposition at high temperature results in an increase and then decreases in deposited material temperature at the interface. The temperature at the center of the deposit (point C) decreased rapidly due to the chilling effect of the former layer at a relatively low temperature. Then it is affected by subsequently deposited material at a high temperature too. However, the cooling rate of position at the center of the deposit is slower than that at the deposit base as it is close to the temperature of surrounding material. Moreover, the highest surface temperature of the deposited material presented at the locations directly facing the spray cone stays is at 820 K (547 °C) in this case (point D).

To verify the modeling of this work, the surface temperature of the deposit at the centerline of the spray cone was measured by an infrared radiation thermometer under a processing condition similar to that for the computation, while the surface temperature of the deposit was measured by a contact pyrometer. Measured temperatures are plotted *vs* time in Figure 6(b) together with the location of the different measurement points, *i.e.*, roller surface and deposit surface. The simulation outcomes had a good agreement with the experimental results. As seen in Figure 6(b), under the standard processing condition the measured surface temperature of deposit was 813 K (540 °C) at 0.62 seconds, which agreed with the calculated value of 820 K (547 °C). The deviation between the simulated and experimental contours is 7 K (−266 °C), is due to the experimental limitations. In the spray rolling process, the temperature cannot be measured accurately. When gas-atomized droplets impinge the substrate or the deposit, a part of droplets was splashed or rebounded away from the deposition surface. The splashed or rebounded droplets lose additional heat, and thus the temperature decreases in the experiment. This can prove the validity of the simplified modeling of deposition by "layered method". Finally, the average temperature of deposit prior to rolling and the corresponding entry angle are determined and utilized to be the initial conditions of rolling.

B. *Cooling Behavior of the Deposited Material During Rolling*

During the rolling stage in spray rolling of 7050 aluminum alloy, the temperature profiles of deposited materials during rolling were presented in Figure 7(a). The simulated surface temperature of strips was 746 K (473 °C) at 0.85 seconds. The surface temperature of the strip surface was measured by a contact pyrometer under a processing condition similar to that for the computation. The measured surface temperature of strips was 738 K (465 °C) at 0.85 seconds, which has a good agreement with the calculation results. The deviations between the simulated and experimental contours depend on the assumed boundary conditions. The used sets of standard boundary conditions are adapted to the measurements with consideration of frequently used data. However, still a large number of free parameters remain.
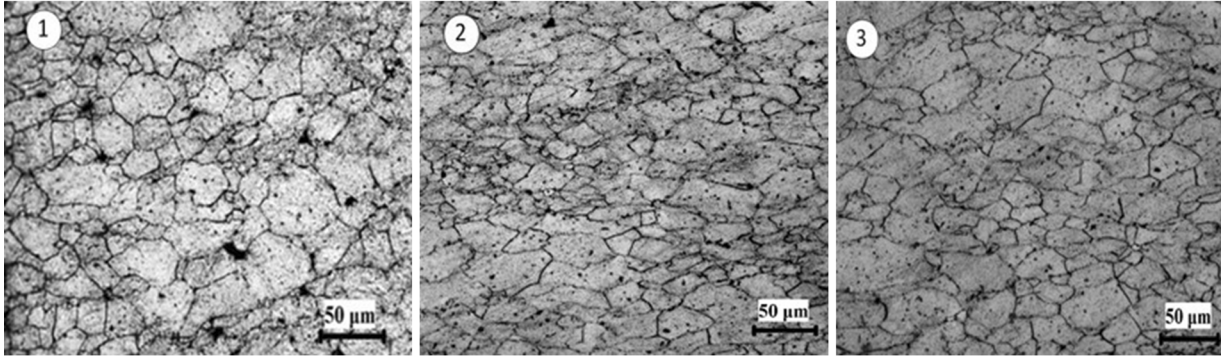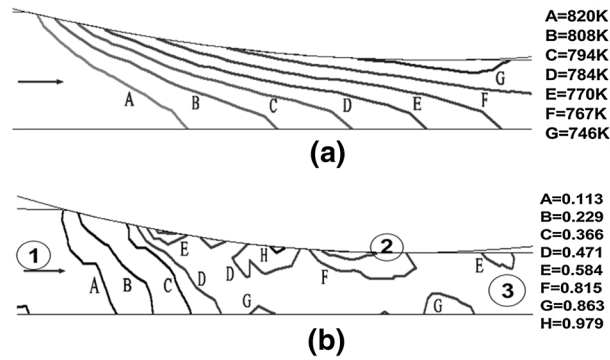
Temperature of the material in the deformation zone decreases from the entry to the exit across the sample section, as well as from the center to the surface (Figure 7(a)). Moreover, it is apparent that the cooling rate at the center is slower than that near the rolling surface. This can be considered to be dictated by the balance between the heat generated as a result of plastic deformation and the rate of heat loss due to conduction, convection, and radiation.

Figure 7(b) shows the total equivalent plastic strain distribution within the deformation zone of the sample. Due to the sudden change of rolling speed in the rolling direction, the lowest total equivalent plastic strain area occurs close to the entry of the roll gap, and subsequently is increasing gradually along the contact arc. In general, the total equivalent plastic strain increases from the center to the surface.

The different solidification behaviors and strain distribution of positions at the center and/or near to the surface are also validated indirectly by the different microstructure characteristics at the surface and center of a rolled strip. The microstructure of spray deposited material prior to rolling exhibits a fine, homogeneous microstructure with equiaxed grain morphology (Figure 7(b)①). And it is also clearly seen that there is a large amount of porosity in the deposited materials. When the rolled strip enters into the deformation region, a state of stress due to roller's friction and pressure is formed near the contact surface with deformation mainly taking place on the deposited material near the rolling surface. This was consistent with dense layer with refined grains distributed near to the contact surface of rolled strips (Figure 7(b)②). It possesses a potential for strain hardening and dynamic recrystallization in the high deformation zone. Comparatively, grains in the center were relatively large and elongated in the rolling direction (Figure 7(b)③). These observations reveal that different microstructural characteristics from the surface to the center of a rolled strip were produced due to the effect of cooling rate and strain distribution in the deformation zone.

IV. DISCUSSION

As we have known, the initial temperature of the droplets, the preheating temperature of the substrate, and the mass flow rate of the spray are very important

(a)

A=820K
B=808K
C=794K
D=784K
E=770K
F=767K
G=746K

(b)

A=0.113
B=0.229
C=0.366
D=0.471
E=0.584
F=0.815
G=0.863
H=0.979

(c)

Fig. 7—Estimated (*a*) temperature and (*b*) total equivalent plastic strain distribution across the sample with microstructures from three locations in the deformation zone: ① deposited material prior to rolling; ② material at the rolling surface; ③ material at the center of the strip.

parameters that affect the thermal profiles of spray-rolled materials. Therefore, the method described above was applied to demonstrate the effect of the processing parameters on thermal profiles of spray-rolled materials. According to the experimental conditions, the typical processing parameters considered in the simulation were as follows: initial droplet temperature ranged from 828 K to 873 K (555 °C to 600 °C) roller preheating temperature ranged from 320 K to 420 K (47 °C to 147 °C) and maximum mass flux in the spray cone m_{max0} ranged from 50 to 30 kg m^{-2} s^{-1}.

As the initial droplet temperature increases, more input enthalpy from the spray to the deposit and the rollers can lead to a higher preform temperature, as shown in Figure 8.

In order to compare with the standard processing condition [an initial droplet temperature of 828 K (555 °C)] in Figure 6, all the parameters are kept constant except the initial droplet temperature [increased to 873 K (600 °C)]. It can be seen obviously that the temperatures of positions at roller surface, deposit base, center of the deposit, and deposit surface are increased. As the initial droplet temperature increases, more residual liquid fraction of impinging droplets is. Although high liquid fraction of the impinging droplets is favorable to increase the relative density of spray rolling aluminum alloy strip, high liquid fraction may cause hot porosity by gas entrapment.[15] However, the porosity can be eliminated by providing a

favorable thickness reduction ratio during the rolling stage. Compared to the standard rolling condition in Figure 7(a), the temperatures of deposited material in the deformation zone increased with increasing initial droplet temperature (Figure 8(b)). An increase in initial droplet temperature results in a slower cooling rate, resulting in a higher temperature for the preform material. The amount of variation of the total equivalent plastic strain of the deposited material in the deformation zone increases with increasing the initial droplet temperature. For example, compared with that for an initial droplet temperature of 828 K (555 °C) (Figure 7(c)), as the initial droplet temperature is increased to 873 K (600 °C) (Figure 8(c)), the highest total equivalent plastic strain area occurring along the contact arc increased from 0.979 to 1.677. Results imply that the deformation of the deposited material during rolling with a large initial droplet temperature is relatively high compared with that with a small one.

Another important parameter of the spray rolling process is the roller surface preheating temperature. As shown in Figure 9(a), the temperature of the deposit is somewhat high as the preheating temperature of the mandrel is increased to 420 K (147 °C). Compared with that for a preheating mandrel temperature of 320 K (47 °C) (Figure 6), the temperatures of positions at roller surface at the same time (at 0.15 seconds) increased by 18 K (−255 °C). Moreover, the temperatures of positions at deposit surface (at 0.62 seconds)
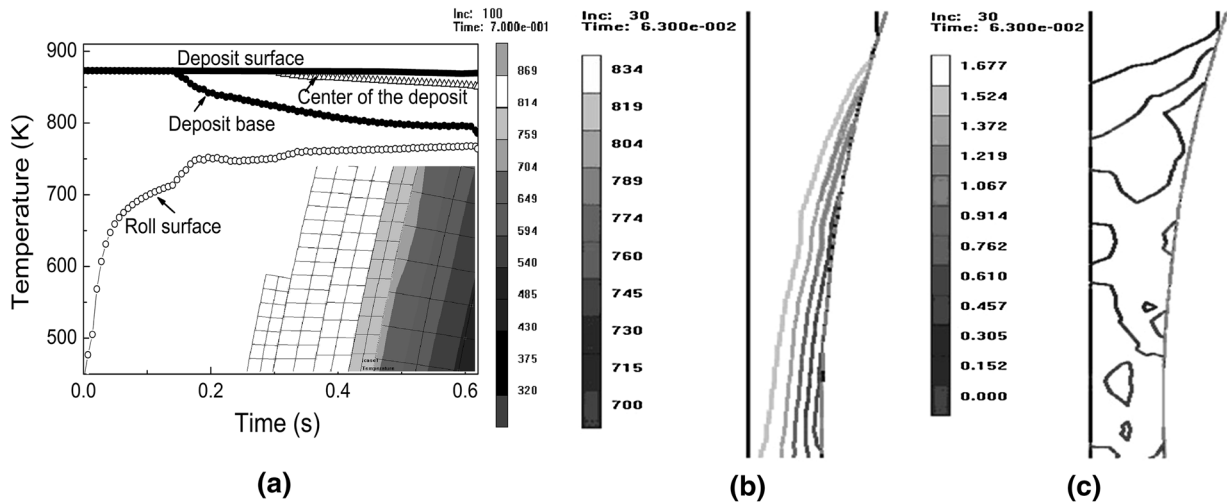
Fig. 8—Effect of initial droplet temperature on the thermal profiles of deposited materials prior to rolling [m = 50 kg m^{-2} s^{-1}, T_{roll} = 320 K (47 °C), and T_d = 873 K (600 °C)]: (*a*) temperature distribution and thermal histories at different positions, (*b*) estimated temperature profiles, and (*c*) the total equivalent plastic strain distribution of deposited materials during rolling.

Fig. 9—Effect of roller preheating temperature on the thermal profiles of deposited materials prior to rolling and during rolling [m = 50 kg m^{-2} s^{-1}, T_{roll} = 420 K (147 °C), and T_d = 828 K (555 °C)]: (*a*) temperature distribution and thermal histories at different positions, (*b*) estimated temperature profiles, and (*c*) the total equivalent plastic strain distribution of deposited materials during rolling.
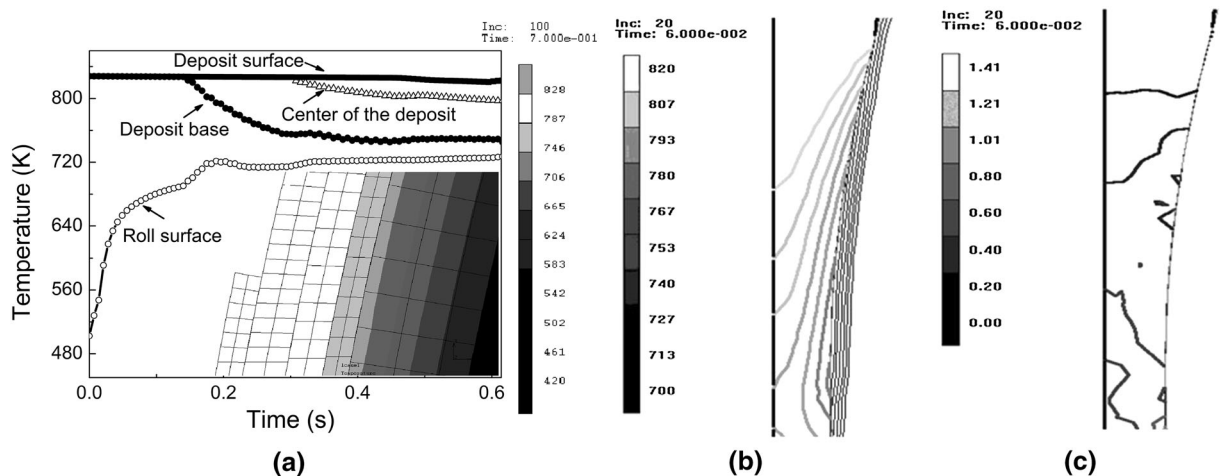
increased by 2.5 K (−270.5 °C). It can be seen that the higher preheating temperature of the mandrel, the less temperature reduced by the gas when the mandrel moves in and out the spray cone is. This approach is expected to produce a homogeneous deposit with uniform solidification behavior during deposition and rolling stage. The distribution of thermal profiles of deposited materials in the thickness direction during rolling is shown in Figure 9(b). Compared to the standard processing condition in Figure 7(a), the temperatures of deposited material in the deformation zone increased with increasing preheating roller temperature (Figure 9(b)). Higher preheating temperature, higher material temperature is. Moreover, the heat generated by friction has only a slight influence on the estimated

temperature. Non-uniformity of total equivalent plastic strain distribution of deposited materials in the deformation zone can be seen in Figure 9(c). Compared with that for a preheating roller temperature of 320 K (47 °C) (Figure 7(b)), the total equivalent plastic strain distribution of deposited material in the deformation zone for a preheating roller temperature of 420 K (147 °C) increases. From this point of view, preheating of the substrate can help avoid fast cooling and eliminate pores of the deposit.

The maximum mass flux in the spray cone (m) has a significant influence on the deposit thickness. A decrease in the maximum mass flux from 50 to 30 kg m^{-2} s^{-1} (Figure 10), a decrease in rolling angle from 0.14 to 0.058 radians is.[13] As shown in Figure 10(a), the
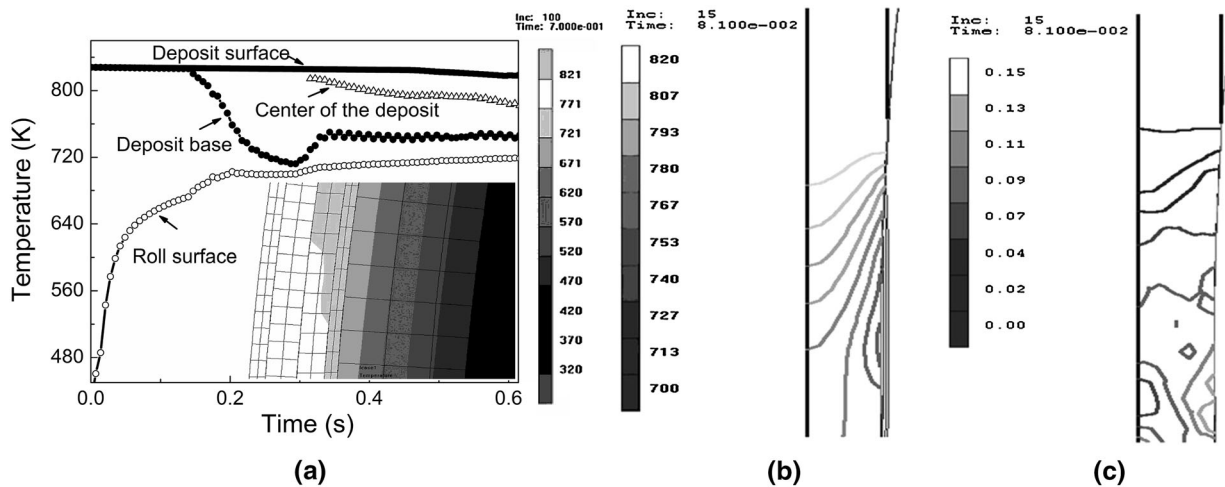
Fig. 10—Effect of maximum mass flux on the thermal profiles of deposited materials prior to rolling and during rolling [m = 30 kg m^{-2} s^{-1}, T_{roll} = 320 K (47 °C), and T_d = 828 K (555 °C)]: (*a*) temperature distribution and thermal histories at different positions, (*b*) estimated temperature profiles, and (*c*) the total equivalent plastic strain distribution of deposited materials during rolling.

temperature of the deposit is low as the maximum mass flux is decreased to 30 kg m^{-2} s^{-1}. Compared with the temperature profile at maximum mass flux of 50 kg m^{-2} s^{-1} (Figure 6), the temperatures of positions at deposit base at the same time (at 0.31 seconds) decreased by 28 K (−245 °C). Moreover, the temperatures of positions at deposit surface (at 0.62 seconds) decreased by 6 K (−267 °C). The temperature decreases due to the convective heat exchange with the surrounding environment and due to the thermal diffusion toward the internal part. Moreover, It is apparent that a lower deposition rate brings less mass heat with little mass input to the deposit, causing the temperature of the entire preform to a lower level. Results imply that the temperature of the deposited material prior to rolling with a large deposition thickness is relatively high compared with that with a small one. In general, the deposition thickness increases with increasing metal mass max flux. The deposition thickness is also sensitive to other process parameters such as the roll gap, the spray distance, the rollers radius, and rotational speed. The deposition thickness becomes larger with decreasing diameter and rotational speed of the rollers and the spray distance and the distance between two rollers.[22] Reduction of the maximum mass flux from 50 to 30 kg m^{-2} s^{-1}, (Figure 10(b)) led to a decrease in temperature of deposited material in the deformation zone. This is attributed to the fact that the deposition thickness is reduced with decreasing maximum mass flux, and a thinner deposition thickness brings less heat with smaller mass input to the deposit. Moreover, due to the less plastic deformation and friction at the contact surface, less heat will be generated when the rolled strips enter into the deformation region. Contact with the roll, under load, provides an efficient conduction path to a heat sink which results in sudden temperature drop of the strip surface. The amount of variation of the total equivalent plastic strain of the deposited material in the deformation zone decreases with decreasing maximum mass flux (Figure 10(c)). This is attributed to different thickness reduction ratios. The thickness reduction ratios for a maximum mass flux of 30 kg m^{-2} s^{-1} decreases to 7.7 pct compared with 40 pct for a maximum mass flux of 50 kg m^{-2} s^{-1}.

The above theoretical and experimental analyses suggest that an increase in preheating roller temperature, initial droplet temperature and maximum mass flux provide a uniform cooling rate prior to rolling contact and during rolling. However, the thermal profiles of the spray-rolled materials are more sensitive to the initial droplet temperature and maximum mass flux from the spray, *i.e.*, the enthalpy and deposition thickness. To increase the relative density of spray-rolled strips, it is proposed to have high deposition thickness and enthalpy remaining in the deposit in the base region. This approach is expected to produce a homogeneous deposit with uniform cooling and solidification behavior in thickness.

However, the simulation accuracy should be further improved. Other processing parameters also have great influence on the thermal history of spray deposit materials during rolling stage, such as the heat-transfer coefficient between the materials and the roller. The developed model of the thermal fields of spray deposited materials on a roller surface has presented a method, analysis, and data to ensure a uniform cooling rate and that assists to improve production rate.

V. CONCLUSIONS

During the spray rolling process, deposition thickness, temperature, and microstructure of deposited materials are parameters to be considered which affect metallurgical quality of the strip. In order to represent the complex thermal history during the spray rolling process, some important physics, such as solid mechanics, thermodynamics, and friction were considered. The heat-transfer models of the deposited material have been established providing the capability to predict the

thermal profiles of the spray-rolled material. The model outcomes had a good agreement with the experimental results. In general, the deposit thickness and enthalpy remaining in the deposit are found to be the dominant influencing factors on producing a homogeneous strip with uniform cooling and solidification condition. The temperature of deposited materials prior to/or during rolling increases with increasing roller preheating temperature, initial droplet temperature, and mass flux distribution of the spray cone. The total equivalent plastic strain distribution in the deformation zone of deposited materials during rolling increased with increasing mass flux, initial droplet temperature, and substrate pre-heating temperature. In this work, a method is presented to ensure a continued operation and homogeneous strip with uniform solidification behavior.

ACKNOWLEDGMENTS

NOMENCLATURE

C_d	heat capacities per unit mass of liquid–solid mixture J kg^{-1} K^{-1}
C_l	heat capacities per unit mass of liquid J kg^{-1} K^{-1}
C_s	heat capacities per unit mass of solid J kg^{-1} K^{-1}
f_l	liquid fraction
f_s	solid fraction
T_l	liquidus temperature K
ΔH_f	latent heat per unit mass J kg^{-1}
ρ	density kg m^{-3}
K	heat conductivity W m^{-1} K^{-1}
T_s	solidus temperature K
ke	coefficient
C_{zong}	equivalent specific heat J kg^{-1} K^{-1}
ρ_{roll}	density of roller kg m^{-3}
C_{roll}	specific heat of roller J kg^{-1} K^{-1}
K_{roll}	heat conductivity of roller W m^{-1} K^{-1}
r	distance from the roller center m
t	time s
T_g	gas temperature K
h_g	heat transfer coefficient at the deposit/gas interface W m^{-2} K^{-1}
q_{con}	heat flux due to gas convective W m^{-2}
q_{em}	heat flux from the preform surface to the environment W m^{-2}
ε	emissivity
σ	Stefan–Boltzmann constant W m^{-2} K^{-4}
T_∞	temperature of the wall of the spraying chamber K
q_{int}	heat flux between the perform and roller W m^{-2}
T_{roll}	temperatures of the roller K
T	temperatures of the interface at the preform side K
h_{int}	heat transfer coefficient at the deposit/substrate interface W m^{-2} K^{-1}
q_{roll}	heat flux from the substrate to the environment W m^{-2}
h_{roll}	heat transfer coefficient at the roller surface W m^{-2} K^{-1}
K_c	thermal conductivity W m^{-1} K^{-1}
K_p	efficiency of conversion of plastic work into heat
$\bar{\sigma}$	equivalent stress N
$\bar{\varepsilon}$	equivalent strain rate ms^{-1}
T_a	ambient temperature K
τ	friction force N
Δv	roller-plate relative velocity ms^{-1}
K_f	distribution coefficient of heat

REFERENCES

1. K.M. McHugh, J.-P. Delplanque, S.B. Johnson, E.J. Lavernia, Y. Zhou, and Y. Lin: *Mater. Sci. Eng. A*, 2004, vol. 383A, pp. 96–106.
2. K.M. McHugh, Y. Lin, Y. Zhou, S.B. Johnson, J.-P. Delplanque, and E.J. Lavernia: *Mater. Sci. Eng. A*, 2008, vol. 477A, pp. 26–28.
3. M.P. Kanouff, R.A. Neiser, and T.J. Roemer: *J. Therm. Spray Technol.*, 1998, vol. 7, pp. 219–28.
4. Z. Djurić, P. Newbery, and P. Grant: *Model. Simul. Mater. Sci.*, 1999, vol. 7, pp. 553–71.
5. N.H. Pryds, J.H. Hattel, T.B. Pedersen, and J. Thorborg: *Acta Mater.*, 2002, vol. 50, pp. 4075–91.
6. J. Mi and P.S. Grant: *Acta Mater.*, 2007, vol. 56, pp. 1588–96.
7. J. Mi and P.S. Grant: *Acta Mater.*, 2007, vol. 56, pp. 1597–1608.
8. C. Cui, U. Fritsching, A. Schulz, and Q. Li: *Acta Mater.*, 2005, vol. 53, pp. 2775–84.
9. P. Mathur, S. Annavarapu, D. Apelian, and A. Lawley: *Mater. Sci. Eng. A*, 1991, vol. 142A, pp. 261–76.
10. M. Buchholz, V. Uhlenwinkel, and N. Ellendt: in *Proceedings of the 4th International Conference on Spray Forming*, A. Leatham, ed., Baltimore, 1999, pp. 13–15.
11. Y. Lin, K.M. McHugh, Y. Zhou, and E.J. Lavernia: *Metall. Mater. Trans. A*, 2004, vol. 35A, pp. 3595–3603.
12. Y. Lin, K.M. McHugh, Y. Zhou, and E.J. Lavernia: *Metall. Mater. Trans. A*, 2004, vol. 35A, pp. 3633–35.
13. F.X. Li, Y.Z. Liu, and X. Luo: *Metall. Mater. Trans. A*, 2012, vol. 43A, pp. 4732–39.
14. J.P. Holman: *Heat Transfer*, 9th ed., McGraw-Hill, NewYork, NY, 2002, p. 8.
15. M.C. Flemings: *Solidification Processing*, MvGraw-Hill, New York, NY, 1974, pp. 34–36.
16. T.P. Battle: *Int. Mater. Rev.*, 1992, vol. 37, p. 249.
17. Q. Xu, V.V. Gupta, and E.J. Lavernia: *Metall. Mater. Trans. B*, 1999, vol. 30B, pp. 527–39.
18. X.T. Li, M.T. Wang, and F.S. Du: *Mater. Sci. Eng.*, 2005, vol. 408A, pp. 33–41.
19. B.Q. Li: *JOM J. Miner. Metall. Mater. S.*, 1995, vol. 47, pp. 29–33.
20. B.Q. Li: *JOM J. Miner. Metall. Mater. S.*, 1995, vol. 47, pp. 13–17.
21. F.X. Li, Y.Z. Liu, W.H. Xiao, and J.L. Xie: *Rev. Adv. Mater. Sci.*, 2013, vol. 33, pp. 291–97.
22. F.X. Li, Y.Z. Liu, J. You, and X. Luo: *Int. J. Adv. Manuf. Technol.*, 2013, vol. 67, pp. 2771–78.